STUDYING SEISMO–ACOUSTIC PROCESSES WITH LASER DEFORMOGRAPHS

A.V.Davydov and G.I.Dolgikh

Pacific Institute of Oceanography,
Far–Eastern Branch of the Russian Academy of Sciences, Vladivostok
Received Mach 18, 1993

This paper deals with estimating the sensitivity of equal– and unequal–arm laser deformographs of various modifications. Estimates account for measurement errors caused by: (1) stability of laser radiation frequency; (2) temperature, humidity, and pressure variations; and, (3) noise of photoelectric devices. It is shown both theoretically and experimentally that in order to increase the sensitivity of deformographs, their supports should be mounted on media with different characteristics and pendulum systems should be used. Some results of correlated measurements with two laser deformographs spaced 250 km *apart are presented.*

In 1979 one of the first laser deformographs in the USSR was created at the Pacific Institute of Oceanography (PIO) of the Far–Eastern Scientific Center of the Academy of Sciences of the USSR under the supervision of Ph.D. U.Kh. Kopvillem. Although at present laser deformographs of the PIO of the Far–Eastern Branch of the Russian Academy of Sciences harness alternative electronic and opto–mechanical base and work on radically different principles, a lot of the credit must go to U.Kh. Kopvillem for development of these instruments and study of their potentialities in the USSR.

Modern laser deformographs measure the shifts of the earth crust to an accuracy of 10^{-10} m in the frequency range up to 10^3 Hz. All the existing laser deformographs may be divided into two classes of equal– and unequal–arm deformographs. Since 1979 the possibilities of using the instruments of both types in the experiments with a modified Michelson interferometer have been investigated comprehensively at the PIO. A comparison between the data obtained in the frequency range up to 10^3 Hz with the use of the equal– and unequal–arm deformographs placed at the Cape Schultz demonstrated that:

(a) sensitivities of both instruments remain identical in the frequency range 1–10^3 Hz;

(b) at frequencies below 1 Hz sensitivity of the unequal–arm deformograph is higher provided both instruments are mounted on uniform base;

(c) differential properties of the base medium, on which the instrument supports are mounted, make it possible to significantly increase the deformograph sensitivity at lower frequencies;

(d) mounting the deformograph reflector on a partially damped pendulum system significantly improves the instrumental sensitivity at high frequencies;

(e) if items (c) and (d) are exactly satisfied, laser deformographs measure practically the absolute shears, and the sensitivities of both types of the instrument become identical.

A choice of an experimental site is of great importance for experiments in the study of seismo–acoustic processes. The sea–land transition zone features the block, irregular, and seismically active structure, in which not only the known signals are resonantly amplified, but also the other linear and nonlinear phenomena are observed. In particular, the use of the laser deformographs in Primorskii Krai made it possible to partially study the structure of the transient zone, its spectral characteristics, and amplification of signals of natural and artificial origin. In addition, the data of deformographs are used to study seismo–acoustic processes of oceanic origin and their transformation at the hydrosphere–lythosphere interface.

SPECIFICATIONS OF THE EQUAL– AND UNEQUAL–ARM DEFORMOGRAPHS AND THEIR POSSIBLE APPLICATIONS

Researchers developing laser deformographs, investigating their applications, and trying to improve their sensitivity, have to pay particular attention to:

1) stability of the laser frequency;

2) account and decrease of the noise of photoelectric units;

3) temperature, baric, and other external effects;

4) design features and placement of the instruments.

In accordance with the foregoing, we consider below the ways of accounting for such factors when operating with the equal– and unequal–arm modifications of laser deformographs.

1. Stability of laser frequency. Since 1979 till 1988 we had performed seismo–acoustic studies with an equal–arm OKG–13 LG–78 105–m laser deformograph without forced frequency stabilization. We now estimate the level of noise due to instability of laser radiation frequency $\Delta\nu/\nu_0$. We define the frequency separation of the fundamental modes of laser oscillations as

$$\Delta\nu = \frac{c}{2nL}, \qquad (1)$$

where c is the speed of light and nL is the optical length of a path between mirrors. The laser cavity being approximately 20 cm long, we find $\Delta\nu = 7.5 \cdot 10^8$ Hz. Let us consider the number of modes that fit into the cavity of a He–Ne laser of length L = 20 cm due to the Doppler effect. First we find the Doppler half–width

0235-6880/93/07 491-06 $02.00

$$\Delta\nu = \frac{2\nu_c}{c}\left(\frac{2\,\kappa T\,\ln 2}{M}\right)^{1/2}, \qquad (2)$$

where ν_c is the frequency of the line center; κ is Boltzmann's constant; M is the atomic mass, in atomic units; and T is the temperature. If we assume that the atomic temperature is of the order of 500 K, the Doppler width of the Ne line for a He–Ne laser generating at a wavelength of 6328 Å will be approximately 1700 MHz. Thus two modes, corresponding to the two axial oscillations, fit into this width, that is, the minimum frequency stability for such a He–Ne laser is controlled by the mode–to–mode transition and is equal to

$$\Delta\nu_D = 1700 \text{ MHz}. \qquad (3)$$

The frequency drift in gas lasers is primarily produced by either mechanical or thermal instabilities of the optical cavity length nL. The above two effects control the actual instability of the operating laser. We define its instability by the expression

$$\frac{\Delta\lambda}{\lambda} = \frac{\Delta(n\,L)}{n\,L}. \qquad (4)$$

Assuming nL to be linear dependent on time within τ_0, we find

$$\frac{\Delta\lambda(\tau_0)}{\lambda} = \frac{\tau_0}{n\,L}\,\frac{\mathrm{d}(n\,L)}{\mathrm{d}t}. \qquad (5)$$

A change in length of the composite cylinders with time may be found from the first order of the thermal expansion coefficients for the materials from which the laser is made. This coefficient for Invar is $5\cdot10^{-7}$ deg^{-1}. Expansion of the laser cylinder is

$$\mathrm{d}L = \alpha_c\,L\,\mathrm{d}\,T \text{ or } \alpha_c = \frac{1}{L}\,\frac{\mathrm{d}\,L}{\mathrm{d}\,T}. \qquad (6)$$

The laser wavelength instability is then equal to

$$\frac{\Delta\lambda(\tau_0)}{\lambda} = \frac{\tau_0\,n\,\alpha_c\,L\,\mathrm{d}\,T}{n\,L\,\mathrm{d}\,T} = \tau_0\,\alpha_c\,\frac{\mathrm{d}\,T}{\mathrm{d}\,t} = 5\cdot10^{-8}, \qquad (7)$$

where τ_0 is the measurement period of the order of 120 hours, while the rate of temperature variation is

$$\frac{\mathrm{d}\,T}{\mathrm{d}\,t} = \pm\,0.1 \text{ deg}/[\tau_0]. \qquad (8)$$

Expression (8) may be written down in terms of $\Delta\nu/\nu$ with allowance for τ_0 and $\mathrm{d}T/\mathrm{d}t$

$$\frac{\Delta\nu}{\nu} = 5\cdot10^{-8}. \qquad (9)$$

Changes in the refractive index of the medium lying between a laser gas–discharge tube and external mirrors are caused by variations in the temperature T, pressure P, and humidity h. Once again, considering only the first order of the coefficients at $T = 293$ K, $P = 760$ Torr, $h = 8.5$ Torr, and $\lambda = 0.63\cdot10^{-6}$ m, we determine the values of the corresponding coefficients

$$\beta_T = \frac{1}{n}\,\frac{\mathrm{d}n}{\mathrm{d}T} = -\,0.3\cdot10^{-7} \text{ deg}^{-1}, \qquad (10)$$

$$\beta_P = \frac{1}{n}\,\frac{\mathrm{d}n}{\mathrm{d}P} = 3.6\cdot10^{-7} \text{ Torr}^{-1}, \qquad (11)$$

$$\beta_h = \frac{1}{n}\,\frac{\mathrm{d}n}{\mathrm{d}h} = 5.7\cdot10^{-8} \text{ Torr}^{-1}. \qquad (12)$$

These expressions are applicable to the part g of the cavity, which is not occupied with the discharge tube (we assume $g = 0.8$). Let the parameters of air inside the laser cavity vary at the rates $\mathrm{d}T/\mathrm{d}t = 0.1^0$/(measurement time) and $\mathrm{d}h/\mathrm{d}t = 0.5$ Torr/(measurement time). Then we obtain

$$\left(\frac{\Delta\lambda_L(t)}{\lambda_L}\right)_{n(T)} = g\,\tau\,\beta_T\,\frac{\mathrm{d}T}{\mathrm{d}t} = \pm\,7.4\cdot10^{-8}, \qquad (13)$$

$$\left(\frac{\Delta\lambda_L(t)}{\lambda_L}\right)_{n(P)} = g\,\tau\,\beta_P\,\frac{\mathrm{d}P}{\mathrm{d}t} = \pm\,8.6\cdot10^{-8}, \qquad (14)$$

$$\left(\frac{\Delta\lambda_L(t)}{\lambda_L}\right)_{n(h)} = g\,\tau\,\beta_h\,\frac{\mathrm{d}h}{\mathrm{d}t} = \pm\,2.28\cdot10^{-8}. \qquad (15)$$

Thus, the stability of laser frequency (neglecting the expansion of the Brewster windows at the ends of the discharge tube and variations in the refractive index of a plasma) is

$$\left(\frac{\Delta\lambda_L}{\lambda_L}\right)_{\text{total}} = \pm\,\{(5)^2 + (7.4)^2 + (8.6)^2 + (2.28)^2\}^{1/2} \times$$

$$\times\ 10^{-8} = 1.26\cdot10^{-8}. \qquad (16)$$

The strain of the deformograph supports is

$$\frac{\Delta l}{l} = -\,\frac{\Delta\lambda}{\lambda}. \qquad (17)$$

If the interferometer arms in the equal–arm configuration are equalized to an accuracy of 10^{-2}, the shear of the interference pattern may be measured to the accuracy $\Delta l = 1.26\cdot10^{-9}$ m for the above–indicated frequency stability. Interferometric techniques used in our deformographs with the equal and unequal arms are capable of measuring the shear of the section of an interference fringe to an accuracy of $\lambda/2\cdot10^{-3}$, where λ is the He–Ne laser wavelength.

Since 1989 seismo–acoustic oscillations have been studied at the PIO FEB RAS using a 52.5–m unequal–arm laser deformograph. In 1991 simultaneous measurements were performed using two unequal–arm laser deformographs, with 52.5–m and 10.5–m arms, spaced 250 km apart. We employed frequency–controlled LGN–303 lasers with long–term stability of 10^{-8} attendant to slow temperature variations within ± 10 K. When the temperature varied within 0.1 K, the laser frequency stability could be improved by 1–2 orders of magnitude. In certain cases an LGN–303M laser was used, whose frequency stability was an order of magnitude higher than that of the LGN–303. Thus, with the above–indicated frequency stabilities of the LGN–303 and LGN–303M, displacements of the supports of the 52.5–m arm deformograph can be measured to the accuracy

$$\Delta l = -\,l\,\frac{\Delta\lambda}{\lambda} = 5.2\cdot10^{-8} - 5.2\cdot10^{-9} \text{ m}, \qquad (18)$$

while those of the 10.5-m arm deformograph – to the accuracy

$$\Delta l = -\, l\,\frac{\Delta\lambda}{\lambda} = 1.05\cdot10^{-8} - 1.05\cdot10^{-9}\ \text{m}\ . \qquad (19)$$

2. Noise of photoelectric equipment. When designing a laser deformograph one has to choose between a photomultiplier and a photodiode as its photodetector. In connection with this we evaluate the noise of a standard photomultiplier PÉU–77 and PD–24K photodiode. Weak variable optical signal is measured by the laser interferometer against a high–level constant background illumination. In this case the minimum threshold sensitivity is determined by the shot noise of the photodetector instead of its dark–current noise. The ratio of the mean–square shot noise of the photomultiplier K_{pm} to the corresponding mean–square value of the photodiode K_{d} is

$$S = \frac{K_{\text{pm}}}{K_{\text{d}}} = \left[\frac{2(1+\beta)\,\Delta f\,\hbar\,\nu}{P_{\text{pm}}\,\eta_{\text{d}}}\right]^{1/2}\left[\frac{2\,\Delta f\,\hbar\,\nu}{P_{\text{pm}}\,\eta_{\text{d}}}\right]^{1/2}, \qquad (20)$$

where β describes the contribution of the secondary electron emission, usually taken to be equal to 1.5; Δf is the reproduced frequency band; $\hbar$ is Planck's constant; ν is the optical radiation frequency; P_{pm} and P_{d} are the powers of illumination of the photocathodes; and, η_{pm} and η_{d} are the quantum efficiencies of these photocathodes. If we assume $\eta_{\text{d}} = 0.6$, $P_{\text{d}} = 10^{-2}$ W, $\eta_{\text{pm}} = 8\cdot10^{-3}$, $P_{\text{pm}} = 7.3\cdot10^{-4}$ W, then $S \simeq 50$. Thus choosing the PD 24K for a photodetector of the laser deformograph is dictated by the preceding.

The intensity of radiation incident on the photodiode I is described by the following expression:

$$I = I_1 + I_2 + 2\sqrt{I_1 I_2}\cos\left[\frac{4\pi(L_2 - L_1)}{\lambda}\right], \qquad (21)$$

where I_1 and I_2 are the intensities of the interfering beams, L_1 and L_2 are the lengths of the interferometer arms, and λ is the He–Ne laser wavelength. For $I_1 = I_2$ we have

$$I = 4\,I_0\cos^2\frac{2\,\pi\,l}{\lambda}, \qquad (22)$$

where $2\,l = 2(L_2 - L_1)$ is the difference between the optical lengths of the paths of the two interfering beams. According to Eq. (22) the output photodetector current is

$$i = i_0\cos^2\frac{2\,\pi\,l}{\lambda}, \qquad (23)$$

where $i_0 = 4I_0\chi$ and χ is the photodetector sensitivity. It follows from Eq. (23) that variations in the output current will be caused by changes in the difference between the optical lengths of the interferometer arms l and by changes in the wavelength λ. In addition noise components appear in the current associated with the noise of photoelectric equipment Δi_1 and instability of the laser output power Δi_2. Differentiating Eq. (23) with respect to l and λ and adding Δi_1 and Δi_2, we obtain

$$\Delta i = i_0\sin\left(\frac{4\,\pi\,l}{\lambda}\right)\left\{\frac{2\,\pi}{\lambda}\,l \pm \frac{2\,\pi\,l}{\lambda^2}\,\Delta\lambda\right\} \pm \Delta i_1 \pm \Delta i_2\ . \qquad (24)$$

The value of Δi is maximum at $4\pi l/\lambda = \pi/2$ and

$$\Delta l = \frac{\Delta i}{i_0}\,\frac{\lambda}{2\pi} \pm l\,\frac{\Delta\lambda}{\lambda} \pm \frac{\Delta i_1}{i_0}\,\frac{\lambda}{2\pi} \pm \frac{\Delta i_2}{i_0}\,\frac{\lambda}{2\pi}, \qquad (25)$$

where $\frac{\Delta i}{i_0}\,\frac{\lambda}{2\pi}$ are seismo–acoustic oscillations and all the other components are noise. Noise due to the instability of the laser frequency $\Delta\lambda/\lambda$ has been analyzed above. For commercial He–Ne lasers the level of relative power fluctuations is about several percent, that is, $\Delta i_2/i_0 \simeq 10^{-2}$. Hence the threshold measurement sensitivity is about 10^{-9} m.

We now estimate the sensitivity threshold due to the shot noise of the photodetector. The minimum threshold sensitivity of the Michelson interferometer with respect to absolute displacements of the mirrors, limited only by the shot noise of the photodetector, is given by the expression (see Refs. 1 and 2)

$$\Delta l_{\min} = \frac{1}{4\pi}\left\{\frac{\lambda\,\hbar\,c\,\Delta f}{q\,P_0}\right\}^{1/2}, \qquad (26)$$

where P_0 is the laser output power, Δf is the receiver bandwidth, and q is the detector quantum yield. Assuming $P_0 = 1\cdot10^{-3}$ W, $q = 0.25$, $c = 3\cdot10^{8}$ m/s, $\lambda = 0.63\cdot10^{-6}$ m, and $\hbar = 6.626\cdot10^{-34}$ J·s, we find

$$\Delta l_{\min} = 1.78\cdot10^{-15}\sqrt{\Delta f}\ \text{m/Hz}^{1/2}\ . \qquad (27)$$

For $\Delta f = 10^3$–10^4 Hz we obtain $\Delta l_{\min}$=$1.78\cdot10^{-13}$ m, so that it has no effect on the measurement accuracy.

3. Thermal, baric, and other effects. Figure 1 shows the block–diagram of the laser deformograph, which can be implemented in two different modifications, namely, with equal arms, when the optical path lengths from the semi–transparent mirror *8* to the reflectors *1* and *2* are equal to each other, and with unequal arms, when the reflector *2* is removed and mirror *10* is set at an angle of 90° relative to the mirror *9* so that the beam reflected from the mirror *10* falls at the point *8* of the semi–transparent mirror. The mirrors *9* and *10* are clamped on piezoceramic cylinders. A 25–kHz driving signal is fed to piezoceramics of the mirror *9*, while piezoceramic of the mirror *10* closes the feedback loop of a recording system, that is, the signal being processed is fed to it.

The plane–parallel mirrors *9* and *10* are clamped on piezoceramic cylinders 10^{-2} m in height. These mirrors are $2\cdot10^{-3}$ m thick. The maximum error in the measurement of a shear reaches $\Delta l = \pm\,0.2\cdot10^{-8}$ m when the temperature varies within ± 0.1 K. The measurement error due to the variations of length of the Invar plate, to which the mirrors *9* and *10* are clamped, may reach $\Delta l = \pm\,0.2\cdot10^{-8}$ m. The total error due to temperature, pressure, and humidity variations within the air gaps of the interferometer is $\Delta l = \pm\,1.1\cdot10^{-9}$ m. When operating with deformograph equipped with air–filled or evacuated tubes, the pressure in the tube must be within ΔP=$2\cdot10^{-10}/0.4\cdot10^{-6} = 5\cdot10^{-4}$ mm Hg, so that to provide the sensitivity $\Delta l/l \sim 2\cdot10^{-10}$. Such variations of pressure in the tube (10^{-4} mm Hg) safely guarantee the necessary measurement accuracy. Now we estimate the temperature variations which would not affect the measurement accuracy

at $P = 10^{-4}$ mm Hg and $\varepsilon = \delta l/l = 2\cdot10^{-10}$. We have $\delta l/l = \alpha\, n_T = 2\cdot10^{-10}\,\Delta T$; whence it follows that $\Delta T = \delta l/(l\cdot2\cdot10^{-6}) = 1$ deg. Thus when the temperature is held at a level of constant ± 0.1 K, this enables us to eliminate the effect of this error on the measurement accuracy.

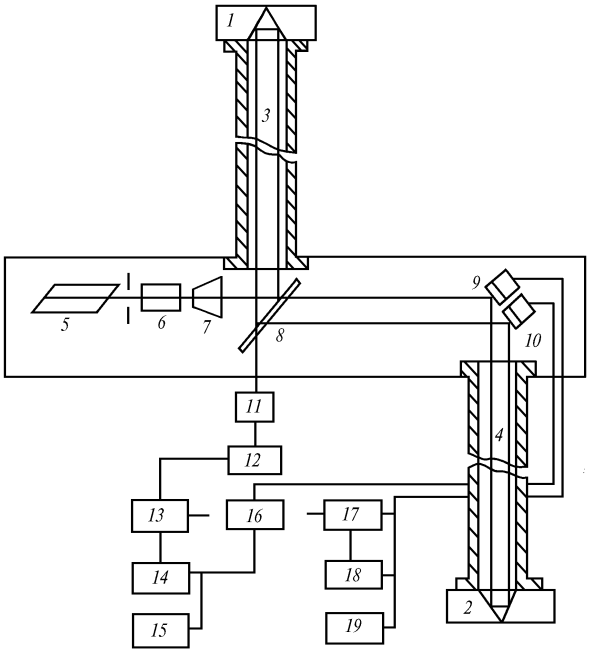

FIG. 1. Block diagram of the laser deformograph: 1 and 2) coner–cube reflectors, 3 and 4) steel light guides, 5) laser, 6) optical shutter, 7) collimator, 8) semi–transparent plate, 9 and 10) plane–parallel mirrors, 11) photodiode, 12) resonance amplifier, 13) synchronous detector, 14) time–delay circuit, 15) reference frequency generator, 16) power amplifier, 17) differential integral amplifier, 18) level reset system, and 19) recording unit.

When one uses evacuated tubes, the change, due to the temperature variations, in the length of the tube used as a vacuum cell will also result in variations of the optical path length, since as the tube elongates, a certain part of the overall beam path in air is substituted by the same path length in vacuum. A temperature change of 10^{-2} K will result in a path length change $\Delta l = \Delta l_0(n - n_0)$, where Δl is the change in the tube length (in case the tube is made of stainless steel we have $\delta l_0 = \alpha l \Delta T = 5.5\cdot10^{-6}$ m) and $(n - n_0)$ is the difference between the refractive indices of air and vacuum. This means that the change in the optical path length is $\Delta l = 5.5\cdot10^{-10}$ m. As can be seen, this interference also does not affect the measurement accuracy.

The change of the tube length due to changes in atmospheric pressure is given by the formula

$$\Delta l = \Delta F\, l/A\, Y\,, \qquad (28)$$

where ΔF is the change in the force of atmospheric pressure exerted at the end of the tube due to the change in the atmospheric pressure; l is the tube length (52.5 m or 10.5 m); A is the cross–sectional area of the tube walls; $\Delta F = \pi r^2 \Delta P$, where r is the tube radius; and, ΔP is the change in the atmospheric pressure. Since $\Delta F = 3.14\cdot10^6$ dyn, $l = 5\cdot10^3$ cm (or $1\cdot10^3$ cm), $A = 19$ cm^2, $Y = 2\cdot10^{11}$ N/m^2, we find $\Delta l = \pi r^2 \Delta P l/AY$, and hence $\Delta l = 5.7\cdot10^{-10}$ m (or $\Delta l = 1.1\cdot10^{-10}$ m).

Making the arms of the laser deformograph equal to each other to an accuracy of 10^{-2} m by mechanical and electro–optical methods, we obtain the error $\Delta l = 0.7\cdot10^{-8}$ m during the measurement period of about 100 hrs. The total error for the two unequal–arm instruments with 52.5–m and 10.5–m arms is $0.8\cdot10^{-8}$ m, respectively. It should be noted that the temperature variations in the thermally insulated cells are less than 0.1 K and are primarily caused by the day–to–day variations in the external temperature. If we limit our studies to seismo–acoustic oscillations within the frequency range 10^{-4}–10^3 Hz, the measurement error decreases by 1–2 orders of magnitude, so that the measurement accuracy correspondingly increases.

4. Constructional and mounting features of the deformograph. Let us consider the response of the medium, on which the laser deformograph is mounted, to a seismo–acoustic wave propagating through this medium. For deformograph of either type with arms oriented along the z axis the measurable displacement is

$$\Delta U = 2U^{(2)} - U^{(1)} - U^{(3)}\,, \qquad (29)$$

where $U^{(1)} = A\,e^{-i\alpha_1 z}\,e^{i(\xi\chi-\omega t)}$, $U^{(2)} = A\,e^{-i\alpha_2(z+L^*)}\,e^{i(\xi\chi-\omega t)}$, $U^{(3)} = A\,e^{-i\alpha_2(z+L^*+L)}\,e^{i(\xi\chi-\omega t)}$, $\alpha_i = \kappa_i \cos\theta_i$, $\kappa_i = 2\pi/\lambda_i$ (i = 1, 2, 3), $L^* \ll L$ for the unequal–arm deformograph; θ_i is the angle of radiation incidence, λ_i is the radiation wavelength in the medium, and $\xi = \kappa_1\sin\theta_1 = \kappa_2\sin\theta_2 = \kappa_3\sin\theta_3$. Below we compare the cases of equal–arm ($L = L^* = 50$ m) and unequal–arm ($L^* = 0.1$ m and $L = 50$ m) deformographs mounted on various media.

Let us consider a homogeneous medium. In this case $\alpha_1 = \alpha_2 = \alpha_3$, $\kappa_1 = \kappa_2 = \kappa_3$, $\theta_1 = \theta_2 = \theta_3$ and $c_1 = c_2 = c_3 = 3$ km/s. As seen from Eq. (29), displacements measured in the low–frequency range ($f > 1$ Hz) differ strongly for the equal– and unequal–arm deformographs mounted on the identical homogeneous media when the incident wave remains the same. Specifically, the sensitivity of the unequal–arm deformograph appears to be much higher than that of the equal–arm deformograph in the frequency range 10^{-2}–10^{-4} Hz. However, the sensitivities of both deformographs are comparable or the sensitivity of the unequal–arm laser deformograph is somewhat higher in the high–frequency range.

Then, following Ref. 3, *we consider two* interfacing *elastic half–spaces with different densities* ρ_1 and ρ_2, longitudinal wave speeds c_1 and c_2, and transverse wave speeds b_1 and b_2. Let the longitudinal wave propagate at the angle θ to the interface through the half–space with larger ρ and c. Let the z axis be oriented perpendicular to the interface and opposite to the incident wave, while the x axis – along the interface. Then, according to Ref. 3, we obtain a system of equations describing the potentials of the longitudinal (φ) and transverse (ψ) waves in half–spaces *1* and *2*

$$\begin{cases} \varphi = \varphi'\,e^{-i\alpha z}\,e^{i(\xi\chi-\omega t)} + \varphi = \varphi''\,e^{-i\alpha z}\,e^{i(\xi\chi-\omega t)}\,, \\ \psi = \psi'\,e^{-i\beta z}\,e^{i(\xi\chi-\omega t)}\,, \end{cases} \qquad (30)$$

$$\begin{cases} \varphi_1 = \varphi_1''\,e^{-i\alpha_1 z}\,e^{i(\xi\chi-\omega t)}\,, \\ \psi_1 = \psi_1'\,e^{-i\beta_1 z}\,e^{i(\xi\chi-\omega t)}\,. \end{cases} \qquad (31)$$

We solve this system with the boundary conditions $[z_z] = 0$, $[z_x] = 0$, $[U_x] = 0$, and $[U_z] = 0$, where z_z and z_x are the components of the stress tensor. In general the displacement U may be found from the expression relating the scalar potential of φ to the vector potential of ψ:

$$\mathbf{U} = \text{grad}\,\varphi + \text{rot}\,\psi\ . \tag{32}$$

From the solution of equations (30)–(32) with the above–indicated boundary conditions we obtain the ratios of the displacements along the z axis in the first and second media

$$\frac{U^{(1)}}{U^{(2)}} = \frac{c_1}{c\,W_l\,l}\ . \tag{33}$$

Solving equations (30)–(33) we find the expressions relating φ', φ'', ψ', φ_1'', and ψ_1''. Let us consider the two media with the following characteristics: $\rho_1 = 2.7$ g/cm^3, $c_1 = 6$ km/s, $\rho_2 = 1.5$ g/cm^3, $c_2 = 1.5$ km/s, $b_1 = 3.5$ km/s, and $b_2 = 0.875$ km/s. The unequal–arm deformograph ($L_1 = 50$ m and $L_2^* = 0.1$ m), when the wave is incident at $\theta = 0°$ with respect to the interface, has two supports separated by a distance of 0.1 m from each other which rest on the medium with the parameters of ρ_1, c_1, and b_1, and the third support located at a distance of 50 m, which rests on the medium with the parameters ρ_2, c_2, and b_2. From Eq. (29) and the solution of Eqs. (30)–(33) we find $\Delta U = 2{\cdot}10^{-5}$ at $f = 10^{-4}$ Hz and $\Delta U = 2{\cdot}10^{3}$ at $f = 10^{-2}$ Hz ($A = 1$); if the angle of incidence is $\theta = 30°$, we have $\Delta U = 7.4{\cdot}10^{-1}$ at $f = 10^{-4}$ Hz and $\Delta U = 6{\cdot}10^{-1}$ at $f = 10^{-2}$ Hz. The equal–arm deformograph ($L = L^* = 50$ m) has two supports which rest on the medium with the parameters ρ_1, c_1, and b_1 and the third support which rests on the medium with the parameters ρ_2, c_2, and b_2. For such a deformograph referring to Eq. (29) and the solution of Eqs. (30)–(33), we find $\Delta U = 1{\cdot}10^{-7}$ at $f = 10^{-4}$ Hz and $\Delta U = 4.4{\cdot}10^{-5}$ at $f = 10^{-2}$ Hz when the radiation is incident at the angle $\theta = 0°$. At $\theta = 30°$ we obtain $\Delta U = -7.4{\cdot}10^{-1}$ at $f = 10^{-4}$ Hz and $\Delta U = -6{\cdot}10^{-1}$ at $f = 10^{-2}$ Hz ($A = 1$).

Let us consider an inhomogeneous layered medium. Then, according to Ref. 4, the expression for the displacement of supports acquires the form

$$U_i^{(n)} = \frac{i\,\kappa_j}{\omega^2\,\rho(n)}\,T_{ij}\,e^{-i\kappa_L z_L^{(n)}}\ , \tag{34}$$

where $n = 1, 2, 3$: $z_L^{(n)}$ are the corresponding coordinates of the supports; T_{ij} is the wave amplitude for the elastic constant tensor. Let us consider the ratios $U_i^{(2)}/U_i^{(1)}$ and $U_i^{(3)}/U_i^{(1)}$ for the equal and unequal–arm deformographs positioned as described above. For the equal–arm deformograph whose first two supports rest on the medium with the density $\rho_1 = 2.7$ g/cm^3 and the third support rests on the medium with $\rho_2 = 1.5$ g/cm^3 we have

$$\frac{U_i^{(2)}}{U_i^{(1)}} \cong e^{-i\kappa_L L}\ ,\quad \frac{U_i^{(3)}}{U_i^{(1)}} \cong \frac{\rho_1\,c_1}{\rho_2\,c_2}\,e^{-i_2\kappa_L L}\ . \tag{35}$$

For very low frequencies $\kappa_L L \ll 1$ we find $U_i^{(2)}/U_i^{(1)} \sim 1$ and $U_i^{(3)}/U_i^{(2)} \sim 7.2$.

The total relative displacement of the supports for both deformographs is determined by the displacement of the supports mounted on the medium with the parameters ρ_2, c_2, and b_2.

Thus, to increase the sensitivity of laser deformographs with the equal and unequal arms, their supports should be mounted on the media with different properties. The relative displacement of the supports of the equal–arm deformograph is equal to that of the unequal–arm deformograph in an ideal model situation.

To improve the laser deformograph sensitivity in the high–frequency range, a physical pendulum with oscillation period $T = 3$ s (i.e., $f_0 = 0.3$ Hz) is mounted on the reflector. For frequencies $f \gg f_0$ the pendulum–mounted reflector suffers practically no displacement. The measurable displacement is then determined by the displacements of the central unit of the deformograph and of the second reflector (for the equal–arm modification). At frequencies close to f_0 the measurable displacement is primarily determined by the displacement of the pendulum–mounted reflector.

MEASUREMENT RESULTS

Here we present some data of measurements with the equal– and unequal–arm laser deformographs (with 52.5–m arm) and compare them. Both deformographs were placed at the Cape Schultz, enclosed in one and the same underground bunker, and rest on the same supports. Measurements with these two instruments were made at different times. Records with identical noise levels (P_0) were selected for further analysis. Table I presents certain comparative results of processing of the data obtained with the equal–arm deformograph (over the periods 15 – 16.09.85 and 24 – 27.09.86) and the data of the unequal–arm deformograph (over the periods 22 – 23.08.91 and 01 – 02.09.91). These data series were subject to harmonic analysis using the Fast Fourier transform (FFT), after the linear trend was estimated and removed.

Since there occur the spectral maxima of various intensity in the frequency ranges of interest, the data segments were further weighted using the 4–term Blackman–Harris window

$$W(n) = 0.35875 - 0.48829\cos\left(\frac{2\pi n}{N}\right) +$$

$$+ 0.14128\cos\left(\frac{4\pi n}{N}\right) - 0.01168\cos\left(\frac{6\pi n}{N}\right),$$

$$y(n) = W(n)\,x(n)\ , \tag{36}$$

so as to suppress the side lobes of the strongest maximum. Here $x(n)$ are the initial data and $y(n)$ are the processed data. This window efficiently suppresses side lobes, so that their level is no more than 74 dB of the principal maximum. Thus in the spectra obtained with the use of such windows the maxima exceeding the level of 70 dB cannot be attributed to side lobes. The program FFT processes the series of 1024 points. If the initial series was shorter (the sampling period was either 1 min or 0.5 min), it was padded with zeros to obtain 1024 point after subtraction of the trend and data processing with the windows.

The problem of selecting the length of a time series for FFT processing is as follows: in the case of a stationary series, the accuracy of reconstruction of the amplitudes and

frequencies of the spectral maxima increases with the period of measurements. However, it has been found from practical experience that seismo–acoustic processes largely fail to comply with the criteria of stationarity. This results in the fact that increase in the length of a record beyond a certain limit (which is different for different frequencies) is futile at best, and sometimes may even decrease the accuracy of reconstruction of the amplitude and frequency of the spectral peak we are interested in. That happens, in particular, when the studied signal is amplitude modulated, or when its frequency (or phase) changes. In connection with this, to study the dynamics of the temporally varying spectral peaks, the length of the analyzed data segments must be shorter than the characteristic time of frequency, amplitude, and phase variations. That is why only 8–14 hrs segments were selected for further analysis. Table I lists several processed segments of records.

TABLE I.

Tone of the Earth's free oscillations (EFO)	From Refs. 5-6	Equal–arm deformograph				Unequal–arm deformograph			
		1985		1986		August 1991		September 1991	
	Period, min	Period, min	log (P/P_0), dB	Period, min	log (P/P_0), dB	Period, min	log (P/P_0), dB	Period, min	log (P/P_0), dB
${}_0S_0$	20.46	20.5	5.1	20.6	8.3	21.3	14.8	20.5	12.9
${}_0S_2$	53.89	53.2	3.6	53.9	9.4	53.9	16.4	53.9	12.5
${}_0S_3$	35.68	36.2	6.7	35.9	8.3	35.6	8.7	35.3	13.7
${}_0S_4$	25.79	26.0	5.7	26.0	4.9	26.2	11.6	24.4	9.8

It can be seen from the table that the amplitudes of low frequency peaks retrieved from the data of the unequal–arm deformograph are 2–3 times as large as those of the equal–arm deformograph. On separate time intervals the amplitudes of maxima are comparable at certain frequencies for both deformographs. We selected only the data with low level of seismo–acoustic background, when local earthquakes and large remote earthquakes were completely absent (only remote earthquakes with the magnitude $M \sim 5$ took place over the measurement period). It follows from the analyses of numerous records of both instruments that the sensitivity of the equal–arm deformograph in the low–frequency range is 2–3 times lower than that of the unequal–arm instrument, while these sensitivities are comparable in the high–frequency range. The significant increase in the sensitivity of the equal–arm deformograph was obtained at the expense of differential properties of the medium during mounting of the instrument.

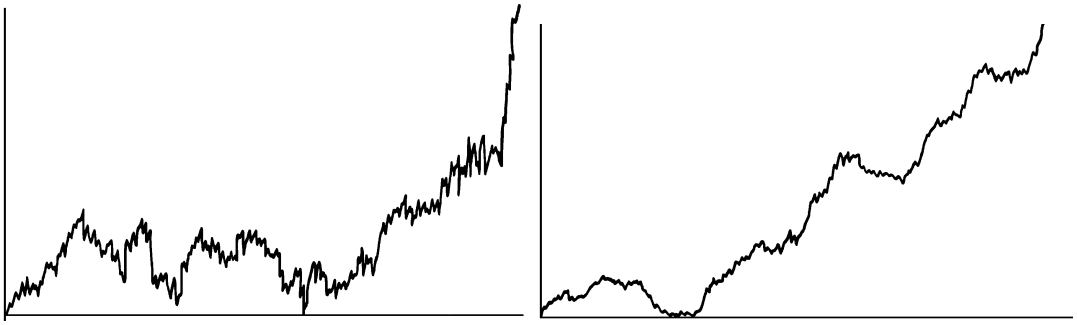

a *b*

FIG. 2. Synchronous sections of records of the deformograph located near Kornilovka (a) and at the Cape Schultz (b). Period of observation is 4 hr 16 min.

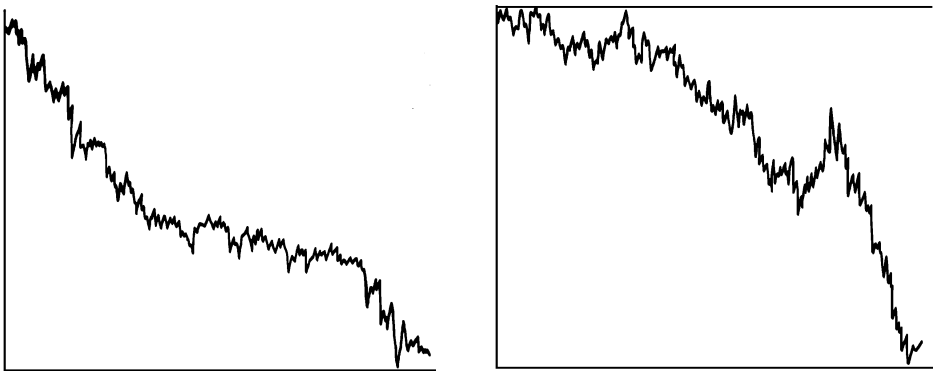

a *b*

FIG. 3. Same as in Fig. 2. Period of observation is 1 hr 06 min.

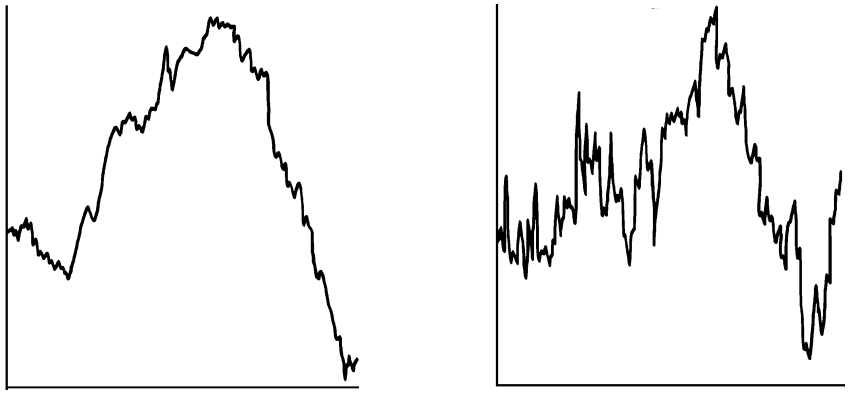

a *b*

FIG. 4. Same as in Figs. 2 and 3. Period of observation is 52 min.

In conclusion we present the data of correlated measurements performed by the two separated unequal–arm laser deformographs. One laser deformograph with the 52.5–m arm was enclosed in a concrete underground bunker located at the Cape Schults. The second 10.5–m arm deformograph was placed on the ground 250 km apart, in village of the Anuchinskii District of Primorskii Krai, and partially thermally insulated. Figures 2–4 show the examples of correlated records of the two instruments for separate time periods obtained with different sampling periods. Comparing these records, we may conclude that:

(1) low–frequency deformation processes in the above–indicated regions are similar in behavior and

(2) records of the 10.5–m arm deformograph feature much stronger high–frequency signals because of ground–based location of this deformograph and stronger effect of anthropogenic interference.

REFERENCES

1. L.F. Vitushkin, M.I. Ivanovskay, and N.I. Kolosnitsyn, Problems in Theories of Gravitation and Elementary Particles, No. 12, 102–111 (1981).
2. L.F. Vitushkin and M.Z. Smirnov, Measurement Techniques **11**, 19–20 (1984).
3. L.M. Brekhovskikh, *Waves in Stratified Media* (Nauka, Moscow, 1973), 343 pp.
4. V.I. Reshetskii, in: *Abstracts of Reports at the Training Seminar on Geophysical Applications of Long–Base Laser Interferometers*, Vladivostok (1987), p. 64–67.
5. A.M. Dziewonski and F. Gilbert, Geophys. J. Roy. Astr. Soc. **27**, 393–446 (1972).
6. J.S. Derr, J. Geophys. Res. **74**, 5202 (1969).